Journal of Organometallic Chemistry, 361 (1989) 409–418
Elsevier Sequoia S.A., Lausanne – Printed in The Netherlands

Insertion of SO_2, CO, or 3,5-$Me_2C_6H_3NC$ into the Pt–O bonds of $Pt(Ph_2PCH_2CMe_2O)$ chelates. Crystal structure of $[PtCl(Ph_2PCH_2CMe_2OCNC_6H_3Me_2$-3,5$)(Ph_2PCH_2CMe_2OH)]$

Nathaniel W. Alcock, Andrew W.G. Platt, Harold H. Powell, and Paul G. Pringle *

Department of Chemistry, University of Warwick, Coventry CV4 7AL (Great Britain)

(Received June 22nd, 1988)

Abstract

Treatment of the *trans*-complex $[PtCl(Ph_2PCH_2CMe_2O)(Ph_2PCH_2CMe_2OH)]$ (**1a**) with Y (Y = SO_2, CO, or 3,5-$Me_2C_6H_3NC$) gives the insertion products *trans*-$[PtCl(Ph_2PCH_2CMe_2OY)(Ph_2PCH_2CMe_2OH)]$ (**3**, **4** and **5**), respectively. The crystal structure of **5** has been determined by X-ray diffraction (R = 0.051 for 2395 observed ($I/\sigma(I) \geq 3.0$) reflections) (Pt–Cl 2.391(6), Pt–P 2.324, 2.281(4), Pt–C 1.978(2) Å). Treatment of the *cis*-complex $[Pt(Ph_2PCH_2CMe_2O)_2]$ (**2**) with SO_2 gives the bis-insertion adduct *trans*-$[Pt(Ph_2PCH_2CMe_2OSO_2)_2]$ (**6**). Under 30 atm of CO, **2** gives the mono-insertion product *trans*-$[(Ph_2PCH_2CMe_2O)Pt(Ph_2PCH_2CMe_2OCO)]$ (**7**). Similarly 3,5-$Me_2C_6H_3NC$ reacts with **2** to give the mono insertion product *trans*-$[(Ph_2PCH_2CMe_2O)Pt(Ph_2PCH_2CMeOCNC_6H_3Me_2$-3,5$)]$ (**8**). The slowness of the reaction of CO with **2** is attributed to steric hindrance by the bulky alkoxo ligand. The mechanism of these insertion reactions is discussed in the light of the relative rates of CO insertion into the Pt–O bonds of *trans*-$[PtX(Ph_2PCH_2CMe_2O)(Ph_2PCH_2CMe_2OH)]$ (X = Cl or CH_3).

Introduction

The insertion of small molecules into late transition metal–alkyl bonds has been exhaustively studied because of its importance in organometallic synthesis and homogeneous catalysis [1]. In contrast, insertions into late transition metal–alkoxo bonds have only recently attracted attention [2], despite the belief that such a reaction is a key step in catalytic processes, such as Pd-catalysed carbonylation of alcohols [3].

* Present address: Department of Chemistry, University of Bristol, Bristol, Great Britain.

0022-328X/89/$03.50

One reason for this neglect has been the observed instability of many alkoxo complexes of the late transition elements [4]. We recently [5] reported the synthesis of chelate alkoxo-platinum complexes whose kinetic stability (to air, moisture and heat) make them convenient compounds for the investigation of alkoxo-platinum chemistry. The insertion of small molecules into the Pt–OR bonds of these chelates are reported below.

Results and discussion

The general reaction studied the ring expansion by insertion of SO_2, CO, or RNC into the chelate alkoxo complexes **1a** or **2**:

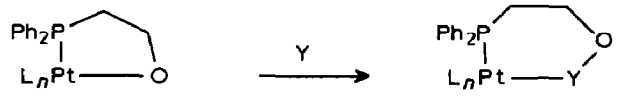

(1)

These reactions can be conveniently monitored by $^{31}P\text{-}\{^1H\}$ NMR spectroscopy since $\delta(P)$ for the five-membered rings falls in the range 20–50 ppm while for the six-membered rings $\delta(P)$ is in the range 0–15 ppm (see Table 1); the high frequency shift of 5-membered chelate phosphine complexes is well known [6]. In addition, infrared spectroscopy was useful for detecting the insertion of the molecules (see Table 1).

Treatment of the *trans*-chelate **1a** with SO_2 (1 atm), CO (1 atm), or 3,5-$Me_2C_6H_3NC$ (1 equiv.) in $CDCl_3$ gave the insertion products **3**, **4** and **5**, respectively, as the major (> 90%) species present in solution. The $^{31}P\text{-}\{^1H\}$ NMR spectra of **3**–**5** (Table 1) each show an AB pattern with ^{195}Pt satellites. The ring expansion (eq. 1) is indicated by the absence of signals in the 20–50 ppm range (see above) and

Table 1

$^{31}P\text{-}\{^1H\}$ NMR [a] and infrared data [b]

	$\delta(P_A)$ (ppm)	$^2J(PtP_A)$ (Hz)	$\delta(P_B)$ (ppm)	$^1J(Pt_AP_B)$ (Hz)	$^2J(P_AP_B)$ (Hz)	IR bands (cm^{-1})
1a	31.0	2937	12.2	2864	454	
1b	38.5	3201	18.3	3137	441	
2	23.9	3308				
3	11.1	2723	1.8	2623	415	
4	12.3	3005	0.8	2783	401	ν(PtCl) 285
						ν(CO) 1640, 1605,
5	9.0	2714	−2.3	2580	313	
	8.6	2662	−2.5	2726	340	
6	4.6	2723				$\nu(SO_2)$ 1370, 1360,
7	35.9	3121	13.4	3142	388	ν(CO) 1627
8	47.5	2338	14.3	2484	362	
9	23.5	3367				
	23.0	3377				
10 [c]	4.2	1886				ν(CO) 1668, 1640
11 [c]	7.0	2898				

[a] A 36.4 MHz in $CDCl_3$. Chemical shifts are in ppm (±0.05) to high frequency of 85% H_3PO_4. Coupling constants are in Hz (±5 Hz). [b] Spectra measured as CsCl discs. [c] The signals for the two diastereoisomers were not resolved.

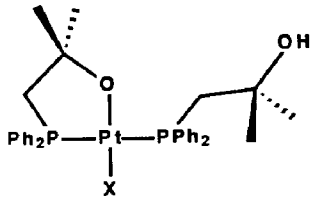

1a X = Cl

1b X = CH_3

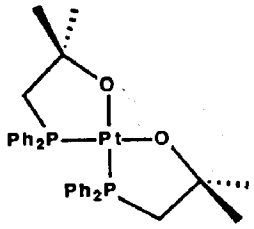

2

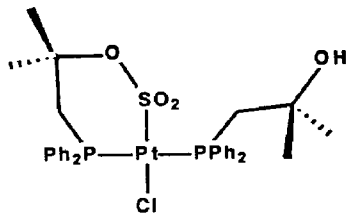

3

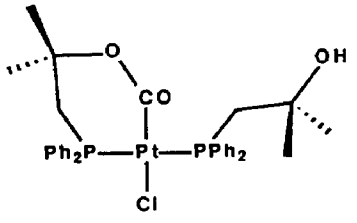

4

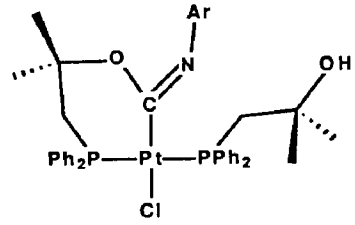

5a

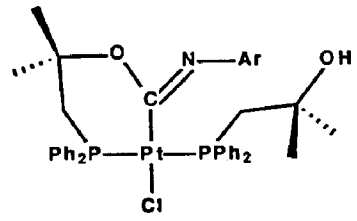

5b

the *trans*-geometry is shown by the large ^2J(PP). Further characterisation of the adducts **3–5** comes from the IR spectra, which show bands in the 270–300 cm^{-1} range assigned to ν(Pt–Cl) and bands assigned to ν(CO) or $\nu(SO_2)$ (see Table 1).

The ^{31}P-{^1H} NMR spectrum of the isocyanide adduct **5** showed the presence of two closely-related species in the ratio 3/2 (see Table 1). These are probably the *cis*/*trans* isomers **5a** and **5b**.

X-ray crystal structure of 5a. The crystal structure of the isocyanide insertion product **5** was determined in order to confirm its identity and give information about the geometry about the CN bond. Figure 1 shows a view of the molecule, and Table 2 lists selected dimensions. The study confirmed the proposed structure (Fig.

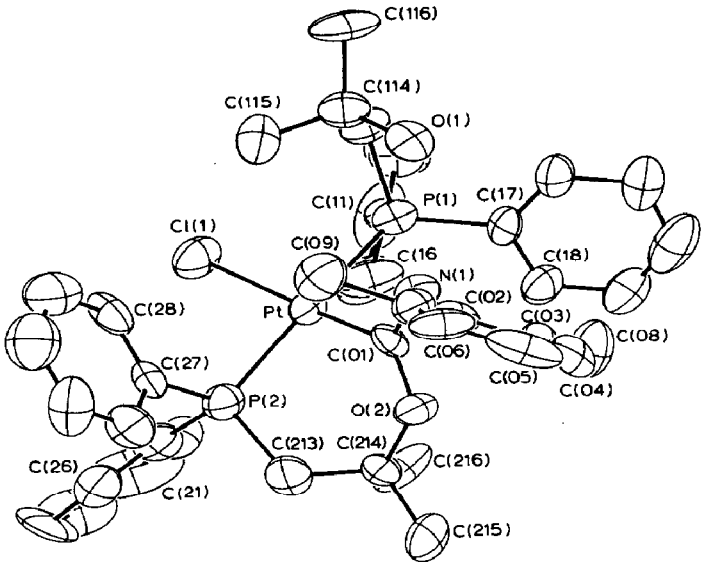

Fig. 1. View of the molecule showing atom numbering (H atoms omitted for clarity).

1), and showed that the square-planar Pt retains the *trans*-coordination of **1a**, with C(01) from the isocyanide inserted into the ring. The chelate ring is close to planar, with the CN inclined to it (torsion angle P(1)–Pt–C(01)–N(1) 57.4(5)°). The C–N bond length (1.31(2) Å) confirms its double-bond character, though the attached groups are slightly twisted out of the expected plane (torsion angle Pt–C(01)–N(1)–C(02) 163.4(8)°). The molecular dimensions are standard (Table 2).

Bubbling of SO_2 through a $CDCl_3$ solution of the *cis*-alkoxo complex **2** gave the bis-insertion product **6**, which was characterised by elemental analysis and ^{31}P-{^1H}

Table 2

Selected bond lengths (Å) and angles (°)

Pt–Cl(1)	2.391(6)	Cl(1)–Pt–P(1)	87.4(2)
Pt–P(1)	2.324(4)	Cl(1)–Pt–P(2)	91.6(2)
Pt–P(2)	2.281(4)	Cl(1)–Pt–C(01)	170.4(5)
Pt–C(01)	1.97(2)	P(1)–Pt–P(2)	174.6(2)
P(1)–C(11)	1.83(2)	P(1)–Pt–C(01)	94.3(4)
P(1)–C(17)	1.79(2)	P(2)–Pt–C(01)	87.6(4)
P(1)–C(113)	1.83(2)	Pt–P(1)–C(11)	109.6(4)
P(2)–C(21)	1.78(2)	Pt–P(1)–C(17)	119.0(5)
P(2)–C(27)	1.79(2)	Pt–P(1)–C(113)	114.1(6)
P(2)–C(213)	1.82(2)	Pt–P(2)–C(21)	117.3(5)
C(01)–O(2)	1.36(2)	Pt–P(2)–C(27)	114.1(4)
C(2)–C(214)	1.41(2)	Pt–P(2)–C(213)	109.7(6)
C(214)–C(213)	1.51(3)	Pt–C(01)–O(2)	127.0(9)
C(01)–N(1)	1.31(2)	Pt–C(01)–N(1)	117.7(11)
N(1)–C(02)	1.42(2)	O(2)–C(01)–N(1)	114.9(14)
		C(01)–O(2)–C(214)	123.5(13)
		O(2)–C(214)–C(213)	109.4(14)
		C(214)–C(213)–P(2)	115.3(11)
		C(01)–N(1)–C(02)	120.0(12)

NMR and IR spectroscopy (Table 1). The *trans* geometry is assigned on the basis of a virtual triplet observed for the ^1H resonance of the CH_2 protons (data in Experimental section). Hence the insertions are accompanied by a *cis* → *trans* change in geometry.

Complex **2** does not react with CO under ambient conditions (1 atm, 25 °C), but under more forcing conditions (30 atm, 25 °C) reaction does take place, and the major species present in solution can be assigned structure **7** on the basis of its solution IR spectrum (ν(CO) at 1627 cm^{-1}) and its ^{31}P-{^1H} NMR spectrum (Table 1), which shows an AB pattern with ^2J(PP) 388 Hz indicating *trans*-phosphines, and $\delta(P_A)$ 35.9 ppm consistent with a phosphorus in a 5-membered chelate ring. Complex **7** was not isolated pure, always being contaminated with **4** (characterised by its ^{31}P spectrum). Complex **4** was the major product when **2** was treated with CO at 80 atm for 3 h; **4** is presumably formed by a reaction involving the solvent ($CDCl_3$). There was no evidence for the formation of a double CO-insertion adduct analogous to **6**.

The reaction of **2** with the bulky isocyanide 3,5-$Me_2C_6H_3NC$ resembles that of **2** with CO. Thus addition of one equivalent of isocyanide to **2** gives the mono-insertion product **8** in essentially 100% yield (characterised by ^{31}P-{^1H} spectroscopy; (see Table 1). Attempts to make double insertion adducts by treatment of **2** with an excess of isocyanide were unsuccessful, complex mixtures of species being produced, some derived from reaction with solvent (e.g. complex **5** was detected).

Bryndza et al. [2] have shown that CO readily inserts under mild conditions into the Pt–O bonds of [(dppe)Pt$(OMe)_2$] to give the complex [(dppe)Pt(CO_2Me)] resulting from double insertion via five coordinate CO complexes. The bidentate phosphine constrains the geometry to *cis* in this case. The reluctance of our *cis*-alkoxo complex **2** to undergo insertion of CO under mild conditions may be due to the fact that the bulk of the alkoxo ligand hinders the formation of a five-coordinate intermediate. The reaction of the less bulky chelate **9** [5] with CO was therefore investigated.

Complex **9** reacts rapidly with CO under mild conditions (1 atm, 20 °C) to give a mixture of two species in approximately equal amounts. These species are assigned structures **10** and **11** on the basis of the IR spectrum of the mixture (ν(CO) 1668, 1640 cm^{-1}), elemental analysis (see Experimental Section), and in particular, the ^{31}P-{^1H} NMR spectrum. The *cis* complex **10** is unambiguously identified by the singlet at 4.2 ppm with small ^1J(PtP) 1886 similar to that for [(dppe)Pt$(CO_2Me)_2$]. The *trans* isomer **11** is characterised by a singlet at 7.0 with J(PtP) of 2989.

It is of interest to compare the action of CO on **1a** and **7**. Rapid insertion of CO was observed for **1a**, in which the Pt–O bond is *trans* to Cl, whereas insertion of CO was not observed with **7**, in which the Pt–O bond is *trans* to an alkoxycarbonyl. The alkoxycarbonyl ligand in **7** is unusual, and so in order to simplify the comparison, complex **1b** having the Pt–O bond *trans* to a methyl ligand was made; like **7**, complex **1b** does not undergo CO insertion under mild conditions. It is possible that the thermodynamics are unfavourable for the formation of a CO insertion product from **7**, but this seems unlikely in view of the ready formation of the related species **11** (see above). It can therefore be concluded that the *trans* influence of the ligand *trans* to Pt–O is not important in controlling the rate of insertion.

The insertion of CO into M–OR bonds may involve the rate-determining formation of ionic alkoxides. Such species have been detected on addition of CO to

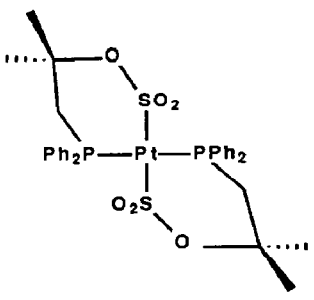

6

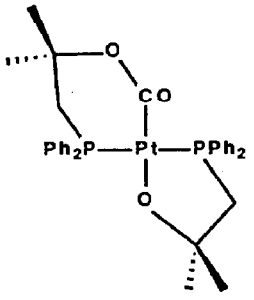

7

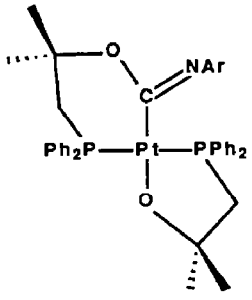

8

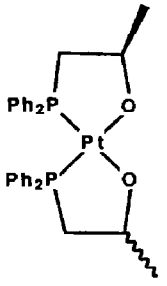

9

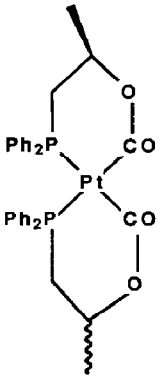

10

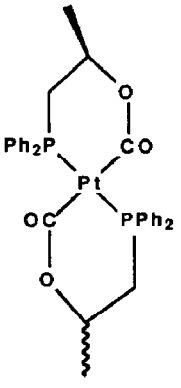

11

alkoxo-iridium(I) complexes [7]. However, our observations above are inconsistent with this mechanism for CO insertion into chelate alkoxo complexes, since weakening of the Pt–OR bond by *trans* labilising ligands would be expected to facilitate insertion involving this dissociative mechanism.

An alternative mechanism involves the rate-determining formation of a five-coordinate complex containing a terminal CO ligand. It would be expected that the greater the Lewis acidity of the four-coordinate precursor, the more favourable this associative mechanism would be i.e. electronegative ligands such as Cl should

increase the overall rate whereas strong σ donors such as CH_3, should reduce it. Since this is what we have observed with our chelates, our results are consistent with the associative mechanism proposed by Bryndza for CO insertions into Pt–O bonds of non-chelate alkoxo complexes.

Experimental

Preparation of trans-[PtCl{$Ph_2PCH_2CMe_2OCN(C_6H_3Me_2$-3,5)}{$Ph_2CH_2CMe_2$-OH}] (5). Complex **1a** (0.108 g, 0.14 mmol) was dissolved in $CDCl_3$ (2.0 cm^3) and 2,5-$Me_2C_6H_3NC$ (0.017 g, 0.17 mmol) added to give a colourless solution. The ^{31}P-{^1H} NMR spectrum of this solution showed quantitative formation of **5**. Crystals of **5** were deposited by slow diffusion of light petroleum b.p. 60–80 °C into this solution. Analysis Found: C, 55.53; H, 5.24; N, 2.05. $C_{41}H_{46}ClNO_2P_2Pt$ calc.: C, 56.1; H, 5.28; N, 1.60%. *Trans*-[PtCl($Ph_2PCH_2CMe_2OCO$)($Ph_2PCH_2CMe_2OH$)] (**3**) and *trans*-[PtCl($Ph_2PCH_2CMe_2OSO_2$)($Ph_2PCH_2CMe_2OH$)] (**4**) were formed by bubbling CO or SO_2 respectively through $CDCl_3$ solutions of **1a**. Neither **3** nor **4** were isolated pure (see Results and discussion).

Preparation of trans-[Pt($Ph_2PCH_2CMe_2OSO_2$)$_2$] · H_2O (6). Sulphur dioxide was bubbled gently through a solution of **2** (0.054 g, 0.07 mmol) in $CDCl_3$ (2.0 cm^3) for 30 min to give a colourless solution, from which the white solid product was precipitated by addition of diethyl ether (10 cm^3). Analysis Found: C, 44.74; H, 4.34. $C_{32}H_{38}O_7P_2PtS_2$ calc.: C, 44.91; H, 4.48%. ^1H NMR data: $\delta(CH_2P)$ 2.91(t) $\delta(CH_3)$ 1.01(s).

Preparation of cis- and trans-[Pt($Ph_2PCH_2CMeHOCO$)$_2$] (10, 11). A solution of complex **9** (0.047 g, 0.07 mmol) in $CDCl_3$ (2.0 cm^3) was saturated with CO. The ^{31}P-{^1H} NMR spectrum of the solution showed that no immediate reaction occurred but after 16 h no starting material remained and the two products **10** and **11** were detected. Precipitation with diethyl ether gave a mixture of these as a pink solid. Analysis Found: C, 51.73; H, 4.90. $C_{32}H_{34}O_4P_2Pt$ calc.: C, 52.11; H, 4.65%.

Under similar conditions the more bulky complex **2** did not react. Complex **2** did react with CO under 30 atm pressure (autoclave) (see Results section).

Preparation of trans-[PtMe($Ph_2PCH_2CMe_2O$)($Ph_2PCH_2CMe_2OH$)] (1b). A solution of [$PtMe_2$(1,5-COD)] (0.065 g, 0.19 mmol) and $Ph_2PCH_2CMe_2OH$ (0.10 g, 0.39 mmol) in toluene (2.0 cm^3) was heated to 100 °C for 1 h to give quantitative formation of the product, which was isolated by removal of the solvent under reduced pressure. Analysis Found: C, 54.39; H, 5.85. $C_{33}H_{40}O_2P_2Pt$ calc.: C, 54.15; H, 5.55%. ^1H NMR data: $\delta(CH_2P)$ 2.69(m), 2.18(m); $\delta(CH_3C)$ 1.23(s), 1.02(s); $\delta(CH_3Pt)$ 0.07(t).

Crystal data. $C_{41}H_{46}ClNO_2P_2Pt$ (excluding solvent) $M = 877.3$, Triclinic, space group $P\bar{1}$, a 9.418(2), b 21.466(4), c 11.832(2) Å, α 107.45(1), $\beta = 108.24(2)$, γ 92.10(2)°, U 2144.7(8) Å^3, $Z = 2$, D_c 1.36 g cm^{-3}, Mo-K_α radiation, λ 0.71069 Å, μ(Mo-K_α) 36.1 cm^{-1}, T 290 K. Needle-shaped white crystals were obtained from $CHCl_3$/petroleum either (b.p. 60–80 °C).

Data were collected with a Syntex $P2_1$ four circle diffractometer. Maximum 2θ was 50°, with scan range ±1.1° (2θ) around the $K_{\alpha1}$–$K_{\alpha2}$ angles, scan speed 3–29° min^{-1}, depending on the intensity of a $2s$ pre-scan; backgrounds were measured at each end of the scan for 0.25 of the scan time. Three standard reflections monitored every 200 reflections showed slight changes, and the data were

Table 3

Atom coordinates ($Å \times 10^4$) and temperature factors ($Å^2 \times 10^3$)

Atom	x	y	z	U^a
Pt	4364.9(7)	2461.2(3)	3891.5(6)	38(1)
Cl(1)	4228(5)	1629(2)	4834(4)	65(2)
P(1)	3720(4)	1615(2)	1973(4)	43(2)
P(2)	5223(5)	3267(2)	5813(4)	50(2)
C(001)	8324(42)	398(18)	6523(34)	67(10)
C(002)	8349(43)	−201(19)	5585(36)	70(10)
C(003)	6982(51)	634(22)	6582(41)	87(12)
O(001)	9422(59)	837(20)	6870(38)	140(13)
O(1)	528(15)	2073(11)	943(15)	56(6)
O(2)	5153(10)	3714(5)	3459(9)	48(4)
N(1)	2825(13)	3156(6)	2293(12)	47(5)
C(01)	4139(17)	3170(7)	3130(12)	40(6)
C(02)	2461(16)	3730(7)	1963(13)	45(6)
C(03)	3073(20)	3940(8)	1158(14)	55(7)
C(04)	2472(24)	4492(8)	814(15)	74(9)
C(05)	1411(22)	4812(8)	1320(18)	87(9)
C(06)	847(17)	4592(8)	2137(18)	65(8)
C(07)	1357(17)	4046(8)	2373(15)	51(7)
C(08)	4160(26)	3612(10)	619(21)	83(11)
C(09)	716(23)	3777(9)	3242(19)	73(10)
C(11)	4936(16)	981(7)	2133(14)	44(6)
C(12)	4469(23)	343(9)	1436(19)	74(10)
C(13)	5416(25)	−126(10)	1476(21)	81(10)
C(14)	6870(32)	64(12)	2336(25)	99(15)
C(15)	7367(24)	718(10)	3105(22)	82(11)
C(16)	6400(19)	1165(8)	2973(19)	70(9)
C(17)	3993(16)	1787(7)	660(13)	42(6)
C(18)	5450(21)	1996(8)	771(16)	59(8)
C(19)	5750(23)	2080(10)	−256(20)	72(10)
C(110)	4678(32)	1995(9)	−1344(26)	93(15)
C(111)	3246(27)	1763(9)	−1546(19)	73(10)
C(112)	2875(21)	1687(9)	−489(15)	63(8)
C(113)	1824(16)	1160(8)	1449(16)	54(7)
C(114)	477(17)	1551(8)	1492(16)	55(7)
C(115)	450(19)	1848(10)	2821(16)	63(8)
C(116)	−953(18)	1056(9)	696(21)	81(10)
C(21)	6587(20)	3087(7)	7062(17)	56(8)
C(22)	7521(16)	2613(11)	6810(17)	73(9)
C(23)	8665(23)	2492(12)	7782(33)	144(20)
C(24)	8812(30)	2907(20)	8840(39)	111(19)
C(25)	8156(28)	3359(11)	9268(18)	111(12)
C(26)	6951(23)	3455(11)	8220(19)	76(10)
C(27)	3780(18)	3523(8)	6460(13)	50(7)
C(28)	2621(18)	3056(10)	6303(14)	62(8)
C(29)	1456(26)	3238(12)	6790(21)	100(12)
C(210)	1445(27)	3901(11)	7447(21)	94(13)
C(211)	2574(27)	4351(11)	7599(20)	87(12)
C(212)	3730(22)	4179(10)	7097(16)	70(9)
C(213)	6139(21)	3992(8)	5689(15)	60(8)
C(214)	6503(17)	3883(8)	4496(13)	53(7)
C(215)	7279(25)	4559(9)	4551(18)	75(10)
C(216)	7592(19)	3367(10)	4276(21)	77(11)

[a] Equivalent isotropic U defined as one third of the trace of the orthogonalised U_{ij} tensor.

rescaled appropriately. Unit cell dimensions and standard deviations were obtained by least-squares fit to 15 reflections ($20 < 2\theta < 22°$).

Reflections were processed by profile analysis to give 3795 unique reflections; 2395 were considered observed ($I/\sigma(I) \geqslant 2.0$) and used in refinement; they were corrected for Lorentz, polarisation, and absorption effects, the last by the Gaussian method; maximum and minimum transmission factors were 0.83 and 0.68. Crystal dimensions were $0.045 \times 0.009 \times 0.24$ mm. There were no systematic absences. The position of Pt with y very close to 0.25 leads to a pseudo-halving of the b axis and to reflections with k odd of low intensity. This doubled b-axis was initially not detected, and reflection data were taken for the sub-cell. Attempts to solve the structure in $P\bar{1}$ ($Z = 1$, Pt at the origin) failed, but a solution was reached in $P1$ with two molecules superimposed.

It was realised that this could be accounted far in terms of the presence of two molecules in a doubled cell. With all k-values doubled, it was not difficult to locate the remaining atoms and identify the gross structure of the molecule (although of course, each new atom on a difference map appeared in two alternative positions, only one of which was correct). Reexamination of the original oscillation photography revealed weak spots corresponding to the reflections from the doubled axis, but it was not possible to recollect the data because the only available crystal had decomposed. Refinement in the doubled cell proved satisfactorily stable. Despite the omission of weak k-odd data, we believe that the structure has been correctly determined, and that no additional information would be gained by re-preparation of the material and recollection of the data.

Anisotropic temperature factors were used for all non-H atoms, except for those of a partly occupied solvent molecule. This was approximated as three C and one O atom at 0.5 occupancy.

H atoms were given fixed isotropic temperature factors, U 0.07 Å^2. Those defined by the molecular geometry were inserted at calculated positions and not refined; methyl and OH H atoms were omitted. Final refinement was on F by cascaded least squares methods refining 49 of parameters. Largest positive and negative peaks on a final difference Fourier synthesis were of height ± 0.6 el, Å^{-3}.

A weighting scheme of the form $w = 1/(\sigma^2(F) = g\delta F^2)$ with $g = 0.003$ was used, and shown to be satisfactory by a weight analysis. Final $R = 0.051$, $R_w = 0.053$. Maximum shift/error in final cycle 0.2. Computing was with SHELXTL [8] on a Data General DG30. Scattering factors in the analytical form and anomalous dispersion factors were taken from International Tables [9]. Final atomic coordinates are given in Table 3, and selected bond lengths and angles in Table 2. Thermal parameters and complete listings of bond lengths and angles and of observed and calculated structure factors are available from the authors.

References

1 J.P. Collman, L.S. Hegedus, J.R. Norton, and R.G. Finke, in Principles and Applications of Organotransition Metal Chemistry, Oxford University Press, 1987.

2 H.E. Bryndza, S.A. Kretchmor, and T.H. Tulip, J. Am. Chem. Soc., 108 (1986) 4805 and ref. therein.

3 H. Alper, B. Despeyroux, and J. Woell, Tetrahedron Lett., 24 (1983) 5691.

4 H.E. Bryndza, L.K. Fong, R.A. Paciello, W. Tam, and J.E. Bercaw, J. Am. Chem. Soc., 109 (1987) 1444.

5 N.W. Alcock, A.W.G. Platt, and P.G. Pringle, J. Chem. Soc., Dalton Trans., (1987) 2273; A.W.G. Platt and P.G. Pringle, J. Chem. Soc., Dalton Trans., in the press.
6 P.E. Garrou, Inorg. Chem., 14 (1975) 1435.
7 W.M. Rees, M.R. Churchill, J.C. Fettinger, and J.D. Atwood, Organometallics, 4 (1985) 2179.
8 G.M. Sheldrick, SHELXTL User Manual, Nicolet XRD Corporation, Madison, Wis. 1983.
9 International Tables for X-Ray Crystallography, Vol. IV, Birmingham, Kynoch Press, 1974.